ACS APPLIED MATERIALS & INTERFACES
Research Article
www.acsami.org

Fast Growth of GaN Epilayers via Laser-Assisted Metal–Organic Chemical Vapor Deposition for Ultraviolet Photodetector Applications

Hossein Rabiee Golgir,[†,⊥] Da Wei Li,[†,⊥] Kamran Keramatnejad,[†] Qi Ming Zou,[†] Jun Xiao,[†] Fei Wang,[‡] Lan Jiang,[§] Jean-François Silvain,[∥] and Yong Feng Lu*[,†]

[†]Department of Electrical and Computer Engineering and [‡]Department of Mechanical & Materials Engineering, University of Nebraska—Lincoln, Lincoln, Nebraska 68588-0511, United States

[§]School of Mechanical Engineering, Beijing Institute of Technology, Beijing 100081, China

[∥]Institut de Chimie de la Matière Condensée de Bordeaux (ICMCB-CNRS), 87 Avenue du Docteur Albert Schweitzer, F-33608 Pessac Cedex, Pessac, France

Supporting Information

ABSTRACT: In this study, we successfully developed a carbon dioxide (CO_2)-laser-assisted metal–organic chemical vapor deposition (LMOCVD) approach to fast synthesis of high-quality gallium nitride (GaN) epilayers on Al_2O_3 [sapphire(0001)] substrates. By employing a two-step growth procedure, high crystallinity and smooth GaN epilayers with a fast growth rate of 25.8 μm/h were obtained. The high crystallinity was confirmed by a combination of techniques, including X-ray diffraction, Raman spectroscopy, transmission electron microscopy, and atomic force microscopy. By optimizing growth parameters, the ~4.3-μm-thick GaN films grown at 990 °C for 10 min showed a smooth surface with a root-mean-square surface roughness of ~1.9 nm and excellent thickness uniformity with sharp GaN/substrate interfaces. The full-width at half-maximum values of the GaN(0002) X-ray rocking curve of 313 arcsec and the GaN($10\bar{1}2$) X-ray rocking curve of 390 arcsec further confirmed the high crystallinity of the GaN epilayers. We also fabricated ultraviolet (UV) photodetectors based on the as-grown GaN layers, which exhibited a high responsivity of 0.108 A W^{-1} at 367 nm and a fast response time of ~125 ns, demonstrating its high optical quality with potential in optoelectronic applications. Our strategy thus provides a simple and cost-effective means toward fast and high-quality GaN heteroepitaxy growth suitable for fabricating high-performance GaN-based UV detectors.

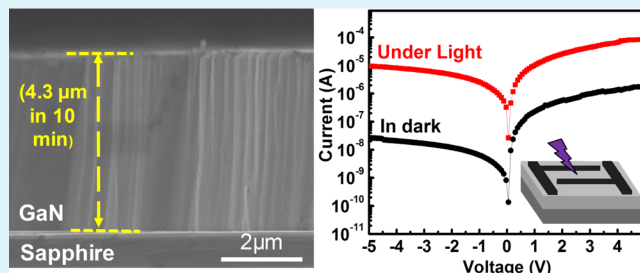

KEYWORDS: *LMOCVD, GaN epilayer, fast growth, ultraviolet photodetector*

Gallium nitride (GaN) with excellent physical properties, such as wide direct band gap, high electron mobility, and high thermal stability, has been extensively studied and attracted attention for applications in light-emitting diodes (LEDs), high-power electronic devices, and short wavelength optoelectronics.[1−3] Current commercial GaN-based devices are fabricated by epitaxy onto foreign substrates because the GaN bulk and freestanding substrate technology is still immature.[4] High-quality GaN are routinely grown by hydride vapor phase epitaxy (HVPE), ammonothermal synthesis, molecular beam epitaxy (MBE), and metal–organic chemical vapor deposition (MOCVD).[5−11] Although HVPE and ammonothermal methods with the advantage of high growth rates have emerged to obtain bulk GaN,[5−7] they lack the precise control and heterojunction layer growth required for device structures. The overwhelming majority of GaN epilayers and GaN-based devices are grown by MOCVD and MBE.[8−12] The MOCVD growth rate of GaN epilayers commonly exceeds 1−3 μm/h, while MBE is typically performed with a growth rate up to 1 μm/h.[8−12] The relatively slow growth rates limit these traditional methods for many device structures that require thick GaN layers. Therefore, synthetic techniques with high growth rates are highly in demand for the scalable production of high-quality GaN epilayers to satisfy the steadily increasing requirement, since it can help reduce the cycle time in device fabrication.

Laser-assisted MOCVD (LMOCVD) is an ideal method for growth of various materials with the advantages of low growth temperature, fast growth rate, and the capability to deposit patterned materials.[13−20] Several semiconductor materials, including silicon, gallium arsenide, indium phosphide, and aluminum nitride, have been successfully grown using LMOCVD.[13−17] For instance, Zhou et al.[21] reported ultraviolet

Received: March 12, 2017
Accepted: June 2, 2017
Published: June 2, 2017

Downloaded via DALIAN UNIV OF TECHNOLOGY on January 11, 2023 at 09:25:42 (UTC).
See https://pubs.acs.org/sharingguidelines for options on how to legitimately share published articles.

ACS Publications © 2017 American Chemical Society

DOI: 10.1021/acsami.7b03554
ACS Appl. Mater. Interfaces 2017, 9, 21539−21547

laser LMOCVD growth of *c*-oriented GaN films with a broad XRD peak at low temperatures. However, the photolysis of the precursors with a UV laser resulted in the low density of the reactive radicals and a slow GaN growth rate. On the other hand, CO_2 laser LMOCVD has been successfully used to prepare various kinds of thin films at high growth rates.[16,22−30] For instance, Iwanaga et al.[22] reported the deposition of large-area amorphous silicon films using CO_2-laser LMOCVD with a high growth rate of >60 μm/h at a relatively low laser power and low substrate temperatures. Recently, we have demonstrated the fast growth of GaN films with (0002) preferential orientation using CO_2-laser LMOCVD with a growth rate up to 84 μm/h at low temperatures,[26] where the experiments were designed to elucidate the GaN growth mechanism via CO_2-laser LMOCVD rather than to optimize the material crystalline quality. The high GaN growth rate is due to the mixed photolysis/pyrolysis reactions of the precursors and the photoinduced effects, as has been evidenced by the wavelength dependence of GaN growth rates.[25−27] However, the low-temperature deposition resulted in films with broad XRD peaks and low crystalline quality.[22,25] The growth of high-quality GaN films suitable for device application were usually realized at high deposition temperatures.[31−34]

In this study, we successfully demonstrated the fast growth of high-quality GaN epilayers on sapphire substrates with a growth rate of 25.8 μm/h using an optimized CO_2-laser LMOCVD method. The growth of GaN epilayers followed previously documented two-step growth steps,[35] including thin three-dimensional (3D) GaN layer growth, lateral growth and coalescence of the 3D layer, and finally quasi-two-dimensional (2D) growth at high temperatures. The growth rate of 25.8 μm/h is 8.6 times higher than that which has been used in GaN epliayers by traditional MOCVD.[11,12] This work presents an efficient and low-cost means to realize fast and high-quality GaN epilayer growth with potential applications in GaN-based optoelectronics.

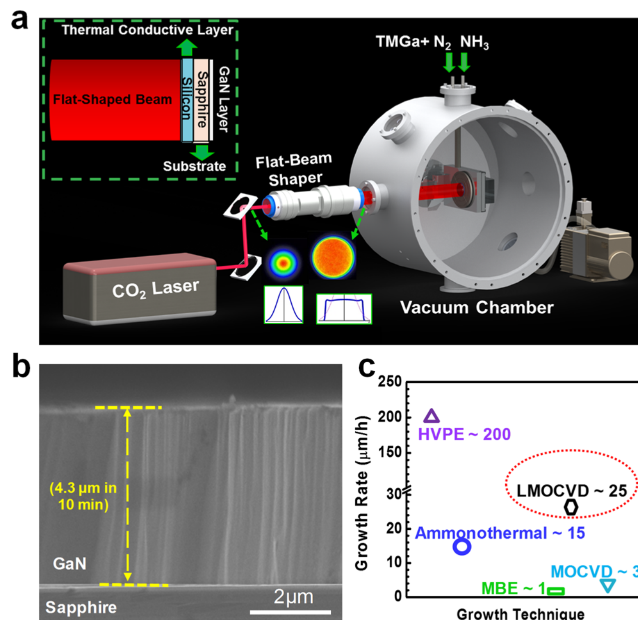

Figure 1. (a) Schematic of the experimental setup of the CO_2-laser LMOCVD system. (b) Cross-sectional SEM image of the ~4.3-μm-thick GaN epilayer grown on a sapphire(0001) substrate at 990 °C for 10 min. (c) A comparison of growth rates between different techniques used for growth of high-quality GaN.

METHODS

Growth of GaN Epilayers. The growth of GaN epilayers on (0001)-orientated sapphire substrates was performed in a homemade vertical LMOCVD system (Figure 1a). Trimethylgallium (TMGa) and ammonia (NH_3) were used as gallium and nitrogen precursors, respectively. The 1 × 1 cm^2 sapphire substrates were successively cleaned in piranha solution and 15% hydrochloric acid solution before loading into the LMOCVD system for the GaN growth. A continuous-wave (CW) and wavelength-tunable CO_2 laser (PRC Inc., λ = 9.201 μm) was used for substrate heating. A flat-top laser beam shaper (Edmund Optics) was used to generate a beam with uniform power distribution (output beam diameter ~20 mm) from a Gaussian CO_2 laser beam (Figure 1a), in order to realize a uniform substrate temperature for material growth with controlled crystal orientations. The chamber pressure during the growth was kept at ~10 Torr. A two-step growth procedure was used for the synthesis of high-quality and smooth GaN epilayers without using AlN buffer layers.[35] NH_3 (26 mmol/min) and TMGa (20 μmol/min) were introduced into the chamber after the substrate temperature was stable under laser irradiation. The growth process started with deposition of a very thin 3D GaN layer (~7−10 nm) for 10 s at 700 °C with a laser power of ~95 W. After that the growth was stopped and the 3D GaN layer was annealed at 990 °C for 5 min (laser power ~160 W) under NH_3 with a flow rate of 26 mmol/min. The subsequent growth of unintentionally doped GaN epilayer was carried out at temperatures ranging from 930 to 990 °C by adjusting the laser power for 10 min. The substrate temperature during the growth was monitored by a pyrometer (Omega, OS3752).

Characterization. The morphology of the GaN layers was investigated using atomic force microscopy (AFM) (Bruker Dimension ICON SPM) and scanning electron microscopy (SEM) (S4700). The structural properties of the GaN epilayers were examined using high-resolution X-ray diffraction (HR-XRD) (Rigaku SmartLab), Raman spectroscopy, and transmission electron microscopy (TEM) (FEI Tecnai OsirisTM, 200 kV). The samples for cross-sectional TEM characterization were prepared as follows. First, the GaN sample was coated with a 20-nm-thick Ti film to prevent ion-beam damage to the sample surfaces during processing with the focused ion beam (FIB). Second, Ga+ ion beams with energies of 30 and 10 keV were used for bulk milling and polishing of Ti-coated GaN sample, respectively, in an FEI Helios NanoLab 660 FIB/SEM system. Finally, the GaN lamellae with a thickness of ~60−100 nm was mounted on the TEM grids. HR-XRD characterization was performed using Rigaku Smart Lab diffractometer with Cu Ka1 radiation (λ = 1.5406 Å). Raman spectra were collected in a micro-Raman system (Renishaw inVia) using a 514.5 nm Ar^+ laser as irradiation source. Hall effect measurements were performed using the Van der Pauw method. Optical transmission spectra were measured via a UV/vis/NIR spectrometer (PerkinElmer LAMBDA 1050).

Fabrication and Characterization of GaN Metal−Semiconductor−Metal (MSM) UV Photodetectors. GaN devices were fabricated using standard photolithography: (1) patterning of the photoresist, (2) deposition of Ni/Au (100 nm/20 nm) for Schottky contact via magnetron sputtering, and (3) lift-off to form Schottky contacts (50 μm long, 10 μm wide with a spacing of 10 μm) on GaN. Before electrical measurement, annealing treatment of GaN MSM devices was performed at 500 °C for 5 min in a rapid thermal processing (RTP) furnace. The current−voltage (I−V) measurements of the GaN UV photodetectors were carried out using a Keithley 237 electrometer. Photoresponse measurements were realized by using a Xe arc lamp with power of 150 W as UV light source. External quantum efficiency (EQE) measurement was performed by using an incident monochromatic light beam directed onto the photodetector, and the data were collected via a Newport QE measurement kit. Transient response measurements were taken using a 337 nm, 4 ns pulsed laser as light source, and voltage variations were collected using an oscilloscope (LeCroy WaveRunner).[36−38] All measurements were conducted at room temperature.

DOI: 10.1021/acsami.7b03554
ACS Appl. Mater. Interfaces 2017, 9, 21539−21547

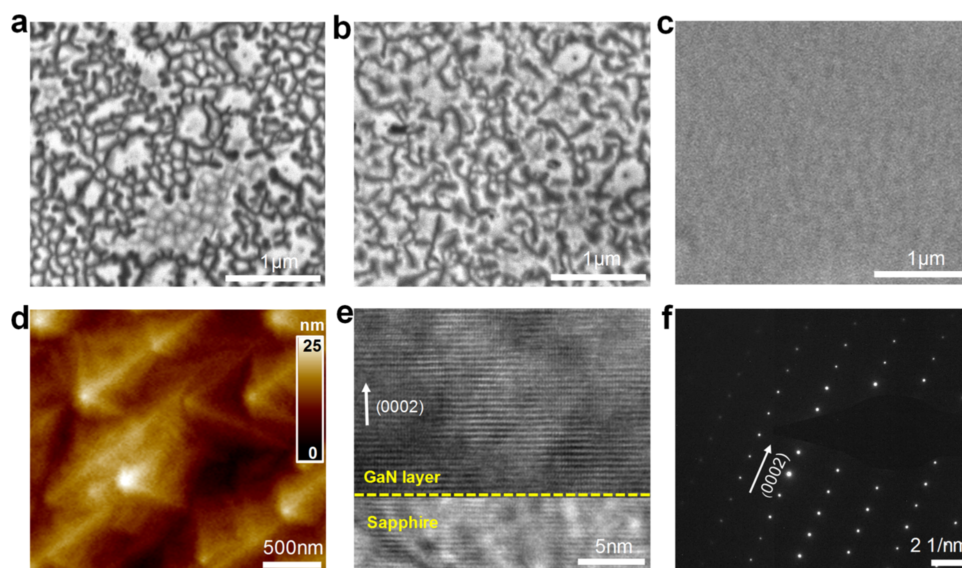

Figure 2. Morphological and structural characterization of GaN epilayers grown on sapphire substrates. SEM plane views of GaN during growth process: (a) GaN islands after 30 s of HT growth, (b) GaN islands after 90 s of HT growth, and (c) GaN epilayers after 10 min of HT growth. (d) AFM image for the GaN epilayer grown at HT for 10 min with an average surface roughness of ∼1.9 nm. (e) High-resolution cross-sectional TEM image for the GaN/sapphire heterointerface. (f) Selected-area diffraction pattern for the GaN epilayer.

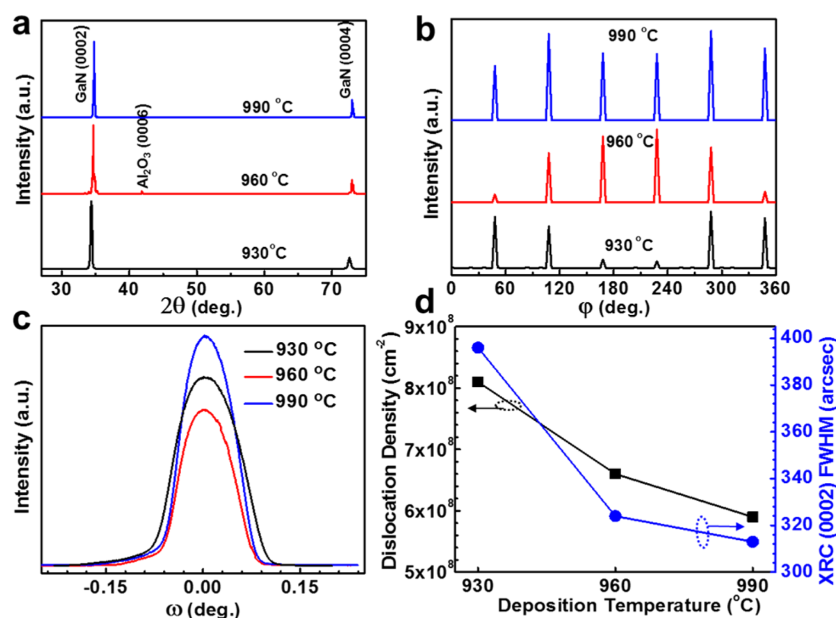

Figure 3. Crystallographic characterization of GaN epilayers grown on sapphire with respect to growth temperatures ranging from 930 to 990 °C. (a) X-ray 2θ scan. (b) X-ray φ scan. (c) XRC curves of the GaN(0002) peak. (d) Temperature dependence of the dislocation density (■) and XRC (0002) FWHM (●) for the GaN epilayers grown on sapphire.

■ RESULTS AND DISCUSSION

Figure 1a shows the schematic LMOCVD system used for fast and high-quality GaN epilayer growth on sapphire substrates. The cross-sectional SEM image in Figure 1b is a typical LMOCVD GaN sample grown at 990 °C for 10 min on sapphire, which shows a very sharp heterointerface between GaN layer and substrate. The thickness of the GaN epilayer was measured to be ∼4.3 μm, corresponding to a growth rate of ∼25.8 μm/h, which is much higher than that of the conventional techniques for GaN epilayer growth (∼1 μm/h for MBE and ∼3 μm/h for MOCVD), as shown in Figure 1c.[8−12] Moreover, the total growth process for LMOCVD was less than 20 min, as compared with several hours needed for the HVPE, ammonothermal, MOCVD, and MBE methods.[5−12] The thicknesses of GaN layers grown at 930 and 960 °C for 10 min were calculated to be ∼3.85 and 4.12 μm, respectively, revealing an increase in growth rates as a function of deposition temperature.

Morphological evolution of GaN during the growth process was investigated, as shown in Figure 2. In step 1, very thin GaN 3D islands with a thickness of ∼7−10 nm were grown at 700 °C. After annealing at 990 °C for 5 min under the NH_3 flow, the GaN islands grew up laterally and started to coalesce gradually. In step 2, with the increasing in the growth time during high temperature (HT) growth, the GaN islands increased in sizes and grew into a continuous and smooth

DOI: 10.1021/acsami.7b03554
ACS Appl. Mater. Interfaces 2017, 9, 21539−21547

Table 1. Summary of Characteristics of the LMOCVD GaN Epilayers Grown on Sapphire at Different Temperatures

no.	temp (°C)	RMS (nm)	band gap (eV)	E_2(high) (cm^{-1})	σ (GPa)	(0002) FWHM (arcsec)	$(10\bar{1}2)$FWHM (arcsec)	dislocation density (cm^{-2})	mobility ($cm^2/V{\cdot}s$)	carrier concn (cm^{-3})
I	930	1.103	3.36	568.7	0.26	396	471	8.1×10^8	226	8.4×10^{16}
II	960	1.253	3.39	571.5	0.82	324	443	6.6×10^8	293	5.3×10^{16}
III	990	1.892	3.38	570	0.47	313	390	5.9×10^8	369	3.1×10^{16}

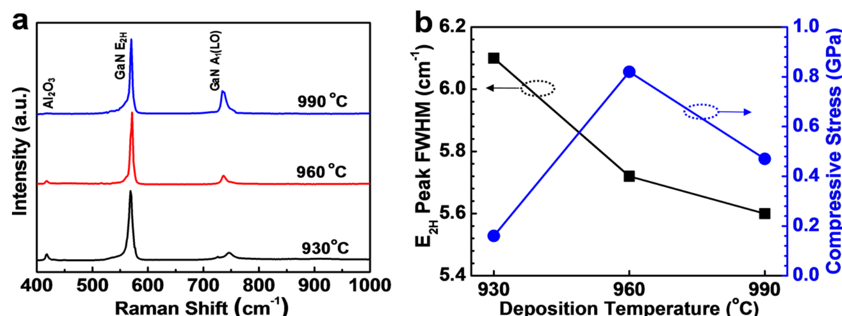

Figure 4. Residual stress evaluation of the GaN epilayers grown on sapphire. (a) Typical Raman spectra of GaN epilayers grown on sapphire at different temperatures. (b) Temperature dependence of the FWHM of the GaN E_2(high) peak (■) and film stresses (●).

film followed by a rapid coalescence.[39] Figure 2a,b shows the top views of GaN islands after 30 and 90 s of HT growth, respectively. It is notable that the sizes and morphologies of the GaN islands are relatively uniform after 90 s of HT growth. The coalescence of GaN islands was completed after ~120 s of HT growth by forming pits with inverted hexagonal pyramid shape (IHP). The IHP defects subsequently disappeared during a further HT growth step (not shown here). Figure 2c shows the SEM image of the GaN epilayers after 10 min of HT growth. It is clear that the 3D island coalescence switched to a 2D step growth mode over the whole substrate. The AFM image of a fully coalesced GaN epilayer in Figure 2d shows a smooth morphology with spiral hillocks, which is similar to that of high-quality GaN grown by the MOCVD and MBE methods with much lower growth rates.[9,40] AFM measurement further revealed that the surface root-mean-square (RMS) roughness for the GaN epilayers grown at 990 °C is as small as 1.892 nm, slightly higher than that of the reported works with much lower growth rates.[9,40,41] GaN with a smooth surface is of great importance for the design and fabrication of high-performance GaN-based optical and optoelectronic devices. The RMS roughness for GaN layers grown at 930 and 960 °C was measured to be 1.103 and 1.253 nm (Figure S1, Supporting Information), respectively, revealing a smoother GaN growth at relatively lower temperatures in this work.

The cross-sectional TEM image of the GaN epilayers grown at 990 °C is shown in Figure 2e. It was observed that the as-grown GaN has a single-crystalline structure with an epitaxial layer even at the interface of GaN and sapphire substrate. The lattice fringes have a spacing of ~0.517 nm, which is consistent with the GaN *c*-plane interplanar distance.[42] The (0002) lattice fringes are parallel to the substrate surface. Figure 2f shows the selected-area electron diffraction (SAED) pattern of the GaN epilayer, which revealed the single crystal array of spots indexed to the reflection of GaN with the wurtzite structure along the (0001) direction. Furthermore, the regularity of the atomic arrangement and the absence of a diffuse streak demonstrated the highly crystalline nature of the GaN epilayers.[42]

XRD was performed to study the structural properties of the GaN epilayers grown on sapphire. Figure 3a compares XRD 2θ scans for the GaN epilayers grown on sapphire at different temperatures. Two peaks at around 34.51 and 72.64 were identified in each spectrum, which are indexed to the reflections of wurtzite GaN(0002) and GaN(0004), respectively. Therefore, the out-of-plane epitaxial relationship of GaN(0001) and sapphire substrate was determined for these samples. Furthermore, it can be observed that the GaN(0002) and GaN(0004) peak intensities are gradually increased and the peaks become sharper as the GaN growth temperature increases from 930 to 990 °C, revealing the improved crystalline quality of the GaN epilayers at higher temperature. An XRD φ scan was conducted to examine the in-plane epitaxial relationship between GaN epilayers and sapphire substrates, while 2θ was constant for the peak position and the GaN sample was rotated 360° around the surface normal. The scanning planes used for the φ scan were hexagonal $(10\bar{1}2)$ and $(11\bar{2}0)$ for GaN layers and sapphire, respectively. Figure 3b shows the normalized φ scans of GaN$(10\bar{1}2)$, where the diffraction peaks with an interval of 60° are observed for all the samples. The variation in the peak intensity versus φ is obvious for each diffraction, which is ascribed to the noncoplanarity of beam vector and surface normal.[43] It has been reported that, in single-crystalline and highly oriented thin films, the diffraction intensity of the planes parallel to the surface is highly sensitive to the GaN sample orientation.[43] Thus, the comparison of the diffraction peak intensity for the samples grown at different temperatures was not performed. Both the XRD 2θ and φ scan results demonstrate that single-crystalline hexagonal GaN epilayers were deposited on the sapphire at temperatures ranging from 930 to 990 °C.

X-ray rocking curve (XRC) is a valid method to evaluate the crystallinity of GaN epilayers. The full width at half-maximum (FWHM) of XRC for the GaN(0002) diffraction peak is used to determine the screw treading dislocations density (TDD) of GaN films, while the FWHM of XRC for the GaN$(10\bar{1}2)$ peak is sensitive to both the edge and screw TDDs.[44] Figure 3c compares the GaN(0002) XRCs for the GaN epilayers grown at different temperatures. The FWHM values of the GaN(0002) and GaN$(10\bar{1}2)$ planes were summarized in Table 1. For the sample grown at 930 °C, the FWHMs of XRC for the GaN(0002) and GaN$(10\bar{1}2)$ diffraction peaks were measured to be 396 and 471 arcsec, respectively, while

DOI: 10.1021/acsami.7b03554
ACS Appl. Mater. Interfaces 2017, 9, 21539−21547

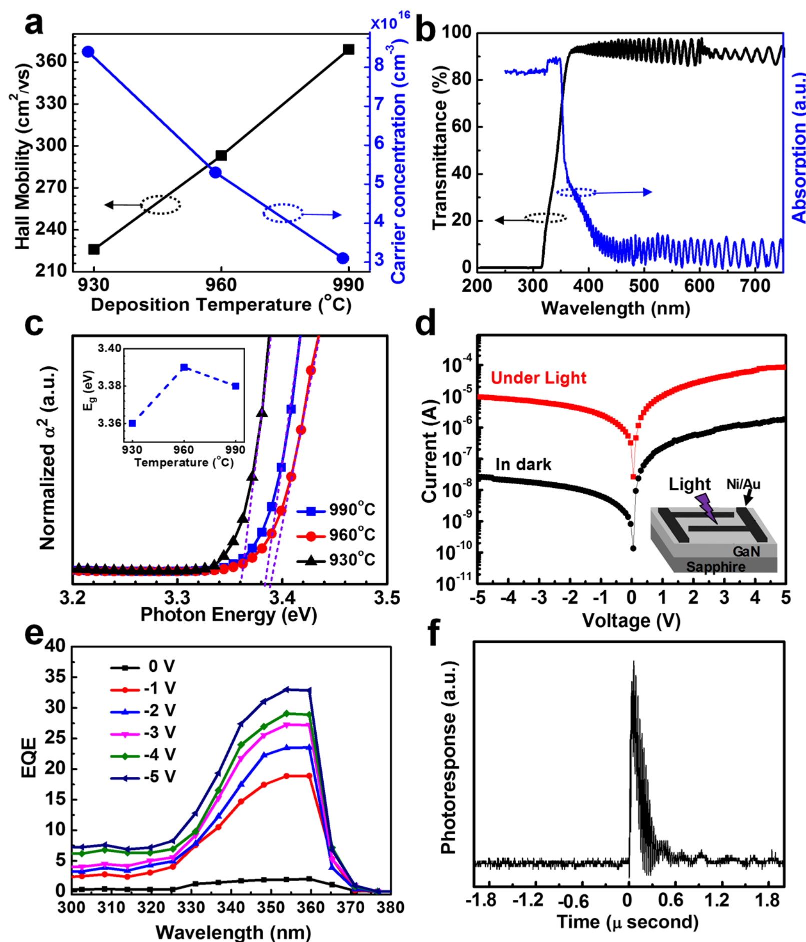

Figure 5. Electrical and optical properties of the LMOCVD GaN epilayers grown on sapphire. (a) Temperature dependence of the Hall mobility (black) and resistivity (blue) of the GaN layers. (b) Transmission and absorption spectra of the GaN layers grown at 990 °C. (c) The optical band gap extracted from part b. (d) $I-V$ curves of a GaN MSM photodetector under light with a power density of 0.1 mW cm^{-2} (red) and in the dark (black). The inset in part d shows the schematic of the device. (e) EQE spectra of the GaN device under a reverse bias from −5 to 0 V. (f) A typical transient photocurrent curve of the GaN device under a reverse bias of −5 V.

these two values monotonously decreased to 324 and 443 arcsec for the GaN grown at 960 °C and further decreased to 313 and 390 arcsec for the sample grown at 990 °C, indicating a higher purity and crystallinity for the GaN epilayers grown at higher temperatures. Note that the low FWHM values obtained at 990 °C are similar to those of GaN epilayers grown using the conventional MOCVD and MBE techniques.[45] The density of dislocations existing in the GaN layers grown at various growth temperatures was calculated using the following equations[44,46]

$$D_{\mathrm{screw}} = \frac{\beta_{(0002)}{}^2}{9b_{\mathrm{screw}}{}^2} \quad D_{\mathrm{edge}} = \frac{\beta_{(10\bar{1}2)}{}^2}{9b_{\mathrm{edge}}{}^2}$$

$$D_{\mathrm{total}} = D_{\mathrm{screw}} + D_{\mathrm{edge}} \tag{1}$$

where D_{screw} and D_{edge} are the screw dislocation density and edge dislocation density, $\beta_{(0002)}$ and $\beta_{(10\bar{1}2)}$ are the FWHM values of XRC for the GaN(0002) and GaN($10\bar{1}2$) peaks, and b_{screw} (0.5185 nm) and b_{edge} (0.3189 nm) are the Burgers vector lengths of GaN. Figure 3d shows the dislocation density of the as-grown GaN epilayers as a function of deposition temperature. The estimated total dislocation densities D_{total} for the samples grown at 930, 960, and 990 °C are 8.1×10^8, 6.6×10^8, and 5.9×10^8 cm^{-2}, respectively. These findings further indicate that the LMOCVD GaN layers grown at higher temperatures have relatively lower crystalline defects.

Raman spectroscopy is a popular method to evaluate the quality and residual stress of nitride films.[47] Figure 4a shows the Raman spectra of GaN epilayers grown at different temperatures. Two prominent phonon modes, E_2(high) and A_1(LO), are observed in each Raman spectrum. The E_2(high) phonon mode is extremely sensitive to the in-plane stress, from which the residual stress in GaN epilayers can be estimated using the following equation[48]

$$\sigma = \frac{\Delta\omega}{4.3(\mathrm{cm}^{-1}\,\mathrm{GPa}^{-1})} \tag{2}$$

where σ and $\Delta\omega$ are the biaxial stress and the shift of E_2(high) peak, respectively. It has been reported that the E_2(high) peak for the stress-free GaN is located at around 567.6 cm^{-1}.[49] The E_2(high) phonon peaks of the GaN films grown at 930, 960, and 990 °C are located at 568.7, 571.5, and 570 cm^{-1}, respectively. The E_2(high) mode peak for all the samples blueshifts compared to that of the stress-free GaN, which suggests that all GaN films suffer from compressive stress, as predicted for the GaN grown on sapphire substrates.[48] It is known that most of the film stresses arise during sample cool down after growth. Figure 4b compares the measured compressive stresses

DOI: 10.1021/acsami.7b03554
ACS Appl. Mater. Interfaces 2017, 9, 21539−21547

in the GaN epilayers grown at different temperatures. The GaN sample grown at 930 °C shows less in-plane compressive stress compared with the samples grown at higher temperatures of 960 and 990 °C. Additionally, the FWHM value of the E_2(high) peak for the GaN epilayers decreased with the increase in the growth temperature, further indicating the high crystallinity of the GaN epilayers grown at higher temperatures.

The electrical and optoelectronic properties of the GaN epilayers were also investigated (Figure 5). Room-temperature Hall effect measurements were performed to study the electrical property of the GaN epilayers, as shown in Figure 5a and Table 1. We found that as the growth temperature increases from 930 to 960 and 990 °C, the mobility increases from 226 to 293 and 369 $cm^2\ V^{-1}\ s^{-1}$ and the carrier concentration decreases from 8.4×10^{16} to 5.3×10^{16} and 3.1×10^{16} cm^{-3}, respectively. The mobility measured in our study is comparable to those reported in several studies for high-quality GaN films deposited using MOCVD and MBE at high temperatures.[50−54] The observed mobility increase with the increased temperature was also reported in the MOCVD GaN films.[53] This can be attributed to the increased film thickness and the improved crystallinity; namely, the crystal defects in the GaN films affect their mobility by scattering the charge carriers.[43,50−54]

The optical transmission and absorption spectra for the GaN epliayers grown at 990 °C are shown in Figure 5b. The absorption coefficient has been determined from optical transmission data (Figure 5c). The band gap, E_g, of semiconductors with direct band gaps can be estimated using the following equation[43,55]

$$\alpha^2 \sim (h\upsilon - E_g) \quad (3)$$

where α is the absorption coefficient, h is Planck's constant, υ is the frequency, and E_g is the semiconductor band gap.[56] The value of the optical band gap can be approximated from a linear extrapolation of the squared absorption, α^2, to the point of interception with the photon energy axis (Figure 5c). As shown in the inset of Figure 5c, the extracted band gaps, E_g, for GaN epilayers grown at 930, 960, and 990 °C are 3.36, 3.39, and 3.38 eV, respectively. These values are slightly smaller than that of bulk GaN.

The optical quality was further evaluated by fabricating a UV photodetector using the as-grown GaN epilayers at 990 °C. GaN UV photodetectors have obtained increasing interest with various applications, such as flame monitoring, biomedicine, and UV astronomy.[57−60] The performance of GaN photodetectors, including responsivity and dark current, is highly dependent on the crystal quality.[61,62] With a high response speed and low dark current characteristics, the GaN MSM photodetector has attracted more attention for UV photodetection applications as compared to GaN photodetectors with other device structures. Additionally, with no n- and p-type doped layers, a GaN MSM device has simple fabrication processes (inset in Figure 5d). Figure 5d compares the current−voltage characteristics of the GaN MSM photodetector in the dark and under light (light intensity ∼0.1 $mW\ cm^{-2}$). The dark current of the photodetector was $\sim 2.7 \times 10^{-8}$ A at a bias voltage of −5 V and increased to $\sim 9.4 \times 10^{-6}$ A under light irradiation, revealing an on/off ratio of ∼348. It is worthwhile to note that the dark current at reverse biases is very low, comparable to that of previously reported GaN UV detectors with the same device structures.[61,62] Figure 5e shows the EQE of the UV detector measured at different reverse biases. The device shows a high sensitivity and high responsivity in the UV range that is near the band edge of GaN. However, the EQE is quickly reduced with either decreasing or increasing wavelength, which is attributed to the increased electron−hole recombination and the reduced photopenetration depth.[36−38,62] The EQE is lower than 2% at a bias of zero, while it increases rapidly as the reverse bias increases and reaches ∼36% at −5 V. The sharp increase of EQE versus reverse bias voltage corresponds to the rapid increase in photocurrent. The responsivity (R) of the device can be measured according to the following equation[37]

$$R = \frac{\text{EQE}}{hc/\lambda} \quad (4)$$

where h is Planck's constant, c is the speed of light, and λ is the wavelength of light. The responsivity peak values of ∼0.0059, 0.069, 0.081, 0.084, and 0.108 $A\ W^{-1}$ were obtained at biases of 0, 1, 2, 3, 4, and 5 V, respectively. The responsivity value of 0.108 $A\ W^{-1}$ is comparable to that of commercial GaN UV photodetectors with values in the range from 0.1 to 0.2 $A\ W^{-1}$.[38,63]

Figure 5f shows the response curve of the GaN UV photodetector measured at a reverse bias voltage of −5 V using a pulsed laser with a wavelength of 337 nm as the light source, from which the response time was extracted to be ∼125 ns. It has been reported that the response time of the device should be limited by the resistor−capacitor time constant but not the GaN crystallinity or carrier mobility.[36] Therefore, the theoretical charge transit time of the UV photodetector was evaluated using the equation below[36]

$$t_e = \frac{L^2}{\mu_e V} \quad (5)$$

where μ_e, t_e, L, and V represent carrier mobility, charge transit time, electrode gap spacing, and applied bias, respectively. Using an electron mobility of 369 $cm^2\ V^{-1}\ s^{-1}$ for the GaN epilayers grown at 990 °C, $L = 10\ \mu m$, and the applied voltage of −5 V, the charge transit time t_e was calculated to be 0.54 ns, which was much lower than the response time of ∼125 ns. The 3 dB cutoff frequency (f_{3dB}) was also estimated from the measured response time t_r of 125 ns using[64]

$$f_{3dB} = \frac{0.35}{t_r} \quad (6)$$

The f_{3db} of the UV GaN photodetector was calculated to be 2.8 MHz. The responsivity of 0.108 $A\ W^{-1}$, fast response time of 125 ns, and f_{3db} of 2.8 MHz for the GaN UV photodetector are comparable to those previously reported in the literature,[61,62] suggesting the excellent optical properties of LMOCVD GaN layers grown with high growth rates.

Although the high-performance UV detectors have been realized on the basis of CO_2-laser LMOCVD of the GaN epilayers, there are still some issues to address for the commercialization of GaN epilayer growth via the LMOCVD technique. For instance, when compared with MOCVD and MBE techniques, the sizes of GaN grown by LMOCVD are relatively small due to the small beam size (20 mm in diameter). By adding a beam expander, the laser beam could be extended to cover whole wafers as well as maintain the required laser fluence for GaN growth, based on which LMOCVD technique is feasible for wafer-scale GaN growth. However, further optimization and design improvement are still required

DOI: 10.1021/acsami.7b03554
ACS Appl. Mater. Interfaces 2017, 9, 21539−21547

to achieve GaN epistructures with a homogeneous thickness and high quality over the whole wafer. Overall, CO_2-laser LMOCVD developed in this work is a simple and low-cost method for fast and high-quality GaN epilayer growth, which might provide an extensive application in electronics and optoelectronics.

■ CONCLUSIONS

In conclusion, we have demonstrated the fast growth of high-quality GaN epilayers with an extremely high growth rate of ~25.8 μm/h via the CO_2-laser LMOCVD method. The deposition temperature is found to be critical in different aspects of as-grown GaN epilayers, including morphology, crystal structure, optical, and optoelectronic properties. The as-grown LMOCVD GaN films have a smooth surface with a RMS roughness of ~1.9 nm. For the GaN samples grown at 990 °C with high growth rates, the FWHMs of the rocking curve ω-scan for the GaN(0002) line and GaN($10\bar{1}2$) lines are 313 and 390 arcsec, respectively, suggesting the high purity and high crystalline quality. A biaxial compressive stress exists in the as-grown GaN epilayers, as has been evidenced by Raman analysis. We have also fabricated UV photodetectors based on the as-grown GaN epilayers, which exhibit a high responsivity of 0.108 A W^{-1} and a fast response time of 125 ns, indicating the excellent optical properties of GaN layers. These results demonstrate that the LMOCVD technique can produce high-quality GaN epilayers with fast growth rates, opening a new pathway for fabrication of nitride-related materials used for next-generation electronics and optoelectronics.

■ ASSOCIATED CONTENT

Supporting Information

The Supporting Information is available free of charge on the ACS Publications website at DOI: 10.1021/acsami.7b03554.

AFM images of the LMOCVD GaN epilayers grown at 930 and 960 °C (PDF)

■ AUTHOR INFORMATION

Corresponding Author

*E-mail: ylu2@unl.edu. Fax: 402-472-4732.

ORCID

Lan Jiang: 0000-0003-0488-1987

Yong Feng Lu: 0000-0002-5942-1999

Author Contributions

⊥H.R.G. and D.W.L. contributed equally to this work.

Notes

The authors declare no competing financial interest.

■ ACKNOWLEDGMENTS

This work was financially supported by the National Science Foundation (NSF CMMI 1129613 and 1265122). Some work was performed in Central Facilities of the Nebraska Center for Materials and Nanoscience, which was supported by the Nebraska Research Initiative.

■ REFERENCES

(1) Akasaki, I.; Amano, H. Breakthroughs in Improving Crystal Quality of GaN and Invention of the P−N Junction Blue-Light-Emitting Diode. *Jpn. J. Appl. Phys.* **2006**, *45*, 9001−9010.

(2) Asif Khan, M.; Bhattarai, A.; Kuznia, J.; Olson, D. High Electron Mobility Transistor Based on a GaN-Al x Ga1− x N Heterojunction. *Appl. Phys. Lett.* **1993**, *63*, 1214−1215.

(3) Ponce, F.; Bour, D. Nitride-Based Semiconductors for Blue and Green Light-Emitting Devices. *Nature* **1997**, *386*, 351−359.

(4) Liu, L.; Edgar, J. H. Substrates for Gallium Nitride Epitaxy. *Mater. Sci. Eng., R* **2002**, *37*, 61−127.

(5) Fujito, K.; Kubo, S.; Nagaoka, H.; Mochizuki, T.; Namita, H.; Nagao, S. Bulk GaN Crystals Grown by HVPE. *J. Cryst. Growth* **2009**, *311*, 3011−3014.

(6) Hashimoto, T.; Wu, F.; Speck, J. S.; Nakamura, S. A GaN Bulk Crystal with Improved Structural Quality Grown by the Ammonothermal Method. *Nat. Mater.* **2007**, *6*, 568−571.

(7) Yamane, H.; Shimada, M.; Clarke, S. J.; DiSalvo, F. J. Preparation of GaN Single Crystals Using a Na Flux. *Chem. Mater.* **1997**, *9*, 413−416.

(8) Tarsa, E.; Heying, B.; Wu, X.; Fini, P.; DenBaars, S.; Speck, J. Homoepitaxial Growth of GaN under Ga-Stable and N-Stable Conditions by Plasma-Assisted Molecular Beam Epitaxy. *J. Appl. Phys.* **1997**, *82*, 5472−5479.

(9) Heying, B.; Averbeck, R.; Chen, L.; Haus, E.; Riechert, H.; Speck, J. Control of GaN Surface Morphologies using Plasma-Assisted Molecular Beam Epitaxy. *J. Appl. Phys.* **2000**, *88*, 1855−1860.

(10) Boyd, A. R.; Degroote, S.; Leys, M.; Schulte, F.; Rockenfeller, O.; Luenenbuerger, M.; Germain, M.; Kaeppeler, J.; Heuken, M. Growth of GaN/AlGaN on 200 mm Diameter Silicon (111) Wafers by MOCVD. *Phys. Status Solidi C* **2009**, *6*, S1045−S1048.

(11) Nakamura, S.; Harada, Y.; Seno, M. Novel Metalorganic Chemical Vapor Deposition System for GaN Growth. *Appl. Phys. Lett.* **1991**, *58*, 2021−2023.

(12) Heikman, S.; Keller, S.; DenBaars, S. P.; Mishra, U. K. Growth of Fe Doped Semi-Insulating GaN by Metalorganic Chemical Vapor Deposition. *Appl. Phys. Lett.* **2002**, *81*, 439−441.

(13) Iga, R.; Sugiura, H.; Yamada, T. Selective Growth of III-V Semiconductor Compounds by Laser-Assisted Epitaxy. *Semicond. Sci. Technol.* **1993**, *8*, 1101−1111.

(14) Shinn, G. B.; Gillespie, P.; Wilson, W., Jr; Duncan, W. M. Laser-Assisted Metalorganic Chemical Vapor Deposition of Zinc Selenide Epitaxial Films. *Appl. Phys. Lett.* **1989**, *54*, 2440−2442.

(15) Allen, S. Laser Chemical Vapor Deposition: A Technique for Selective Area Deposition. *J. Appl. Phys.* **1981**, *52*, 6501−6505.

(16) Herman, I. P. Laser-Assisted Deposition of Thin Films from Gas-Phase and Surface-Adsorbed Molecules. *Chem. Rev.* **1989**, *89*, 1323−1357.

(17) Duty, C.; Jean, D.; Lackey, W. Laser Chemical Vapour Deposition: Materials, Modelling, and Process Control. *Int. Mater. Rev.* **2001**, *46*, 271−287.

(18) Keramatnejad, K.; Zhou, Y. S.; Gao, Y.; Rabiee Golgir, H.; Wang, M.; Jiang, L.; Silvain, J.-F.; Lu, Y. F. Skin Effect Mitigation in Laser Processed Multi-Walled Carbon Nanotube/Copper Conductors. *J. Appl. Phys.* **2015**, *118*, 154311.

(19) Keramatnejad, K.; Zhou, Y.; Li, D.; Golgir, H. R.; Huang, X.; Zhou, Q.; Song, J.; Ducharme, S.; Lu, Y. Laser-Assisted Nanowelding of Graphene to Metals: An Optical Approach Toward Ultralow Contact Resistance. *Adv. Mater. Interfaces* **2017**, 1700294.

(20) Keramatnejad, K.; Rabiee Golgir, H.; Zhou, Y.; Li, D.; Huang, X.; Lu, Y. Reducing Graphene-Metal Contact Resistance via Laser Nano-welding. *Proc. SPIE* **2017**, *10092*, 100921X.

(21) Zhou, B.; Li, Z.; Tansley, T.; Butcher, K. Growth Mechanisms in Excimer Laser Photolytic Deposition of Gallium Nitride at 500° C. *J. Cryst. Growth* **1996**, *160*, 201−206.

(22) Iwanaga, T.; Hanabusa, M. CO_2 Laser CVD of Disilane. *Jpn. J. Appl. Phys.* **1984**, *23*, L473.

(23) Thirugnanam, P.; Xiong, W.; Mahjouri-Samani, M.; Fan, L. S.; Raju, R.; Mitchell, M.; Gao, Y.; Krishnan, B.; Zhou, Y. S.; Jiang, L.; Lu, Y. F. Rapid Growth of M-Plane Oriented Gallium Nitride Nanoplates on Silicon Substrate Using Laser-Assisted Metal Organic Chemical Vapor Deposition. *Cryst. Growth Des.* **2013**, *13*, 3171−3176.

(24) Besling, W.; Goossens, A.; Meester, B.; Schoonman, J. Laser-Induced Chemical Vapor Deposition of Nanostructured Silicon Carbonitride Thin Films. *J. Appl. Phys.* **1998**, *83*, 544−553.

(25) Rabiee Golgir, H.; Gao, Y.; Zhou, Y. S.; Fan, L.; Thirugnanam, P.; Keramatnejad, K.; Jiang, L.; Silvain, J.-F. o.; Lu, Y. F. Low-Temperature Growth of Crystalline Gallium Nitride Films Using Vibrational Excitation of Ammonia Molecules in Laser-Assisted Metalorganic Chemical Vapor Deposition. *Cryst. Growth Des.* **2014**, *14*, 6248−6253.

(26) Golgir, H. R.; Zhou, Y. S.; Li, D. W.; Keramatnejad, K.; Xiong, W.; Wang, M. M.; Jiang, L. J.; Huang, X.; Jiang, L.; Silvain, J. F.; Lu, Y. F. Resonant and Nonresonant Vibrational Excitation of Ammonia Molecules in the Growth of Gallium Nitride Using Laser-Assisted Metal Organic Chemical Vapour Deposition. *J. Appl. Phys.* **2016**, *120*, 105303.

(27) Lu, Y.; Golgir, H. R.; Zhou, Y. Growth of Nitride Films. US Patent 20,160,340,783, 2016.

(28) Meunier, M.; Flint, J.; Haggerty, J.; Adler, D. Laser-Induced Chemical Vapor Deposition of Hydrogenated Amorphous Silicon. I. Gas-Phase Process Model. *J. Appl. Phys.* **1987**, *62*, 2812−2821.

(29) Golgir, H. R.; Gao, Y.; Zhou, Y.; Fan, L.; Keramatnejad, K.; Lu, Y. Effect of Laser-Assisted Resonant Excitation on the Growth of GaN Films. *Proceedings of the 33nd International Congress on Applications of Lasers and Electro-Optics (ICALEO)*; LIA, 2014.

(30) Thirugnanam, P.; Zhou, Y.; Golgir, H.; Gao, Y.; Lu, Y. Synthesis of Gallium Nitride Nanoplates Using Laser-Assisted Metal Organic Chemical Vapor Deposition. *Proceedings of the 32nd International Congress on Applications of Lasers and Electro-Optics (ICALEO)*; LIA, 2013.

(31) Park, M.; Maria, J.-P.; Cuomo, J.; Chang, Y.; Muth, J.; Kolbas, R.; Nemanich, R.; Carlson, E.; Bumgarner, J. X-Ray and Raman Analyses of GaN Produced by Ultrahigh-Rate Magnetron Sputter Epitaxy. *Appl. Phys. Lett.* **2002**, *81*, 1797−1799.

(32) Schiaber, Z. S.; Leite, D. M.; Bortoleto, J. R.; Lisboa-Filho, P. N.; da Silva, J. H. Effects of Substrate Temperature, Substrate Orientation, and Energetic Atomic Collisions on the Structure of GaN Films Grown by Reactive Sputtering. *J. Appl. Phys.* **2013**, *114*, 183515.

(33) Hao, M.; Ishikawa, H.; Egawa, T. Formation Chemistry of High-Density Nanocraters on the Surface of Sapphire Substrates with an In-Situ Etching and Growth Mechanism of Device-Quality GaN Films on the Etched Substrates. *Appl. Phys. Lett.* **2004**, *84*, 4041−4043.

(34) Yadav, B. S.; Major, S.; Srinivasa, R. Growth and Structure of Sputtered Gallium Nitride Films. *J. Appl. Phys.* **2007**, *102*, 073516.

(35) Lahreche, H.; Leroux, M.; Laügt, M.; Vaille, M.; Beaumont, B.; Gibart, P. Buffer Free Direct Growth of GaN on 6H−SiC by Metalorganic Vapor Phase Epitaxy. *J. Appl. Phys.* **2000**, *87*, 577−583.

(36) Fang, Y.; Huang, J. Resolving Weak Light of Sub-Picowatt per Square Centimeter by Hybrid Perovskite Photodetectors Enabled by Noise Reduction. *Adv. Mater.* **2015**, *27*, 2804−2810.

(37) Guo, F.; Xiao, Z.; Huang, J. Fullerene Photodetectors with a Linear Dynamic Range of 90 dB Enabled by a Cross-Linkable Buffer Layer. *Adv. Opt. Mater.* **2013**, *1*, 289−294.

(38) Guo, F.; Yang, B.; Yuan, Y.; Xiao, Z.; Dong, Q.; Bi, Y.; Huang, J. A Nanocomposite Ultraviolet Photodetector Based on Interfacial Trap-Controlled Charge Injection. *Nat. Nanotechnol.* **2012**, *7*, 798−802.

(39) Li, J.; Chen, Z.; Jiao, Q.; Feng, Y.; Jiang, S.; Chen, Y.; Yu, T.; Li, S.; Zhang, G. Silane Controlled Three Dimensional GaN Growth and Recovery Stages on a Cone-Shape Nanoscale Patterned Sapphire Substrate by MOCVD. *CrystEngComm* **2015**, *17*, 4469−4474.

(40) Gunning, B. P.; Clinton, E. A.; Merola, J. J.; Doolittle, W. A.; Bresnahan, R. C. Control of Ion Content and Nitrogen Species Using a Mixed Chemistry Plasma for GaN Grown at Extremely High Growth Rates > 9 μ m/h by Plasma-Assisted Molecular Beam Epitaxy. *J. Appl. Phys.* **2015**, *118*, 155302.

(41) Gibart, P. Metal Organic Vapour Phase Epitaxy of GaN and Lateral Overgrowth. *Rep. Prog. Phys.* **2004**, *67*, 667−715.

(42) Kim, J.; Bayram, C.; Park, H.; Cheng, C.-W.; Dimitrakopoulos, C.; Ott, J. A.; Reuter, K. B.; Bedell, S. W.; Sadana, D. K. Principle of Direct Van Der Waals Epitaxy of Single-Crystalline Films on Epitaxial Graphene. *Nat. Commun.* **2014**, *5*, 4836.

(43) Motamedi, P.; Cadien, K. Structure-Property Relationship and Interfacial Phenomena in GaN Grown on C-Plane Sapphire via Plasma-Enhanced Atomic Layer Deposition. *RSC Adv.* **2015**, *5*, 57865−57874.

(44) Moram, M.; Vickers, M. X-Ray Diffraction of III-Nitrides. *Rep. Prog. Phys.* **2009**, *72*, 036502.

(45) Collazo, R.; Mita, S.; Aleksov, A.; Schlesser, R.; Sitar, Z. Growth of Ga-and N-Polar Gallium Nitride Layers by Metalorganic Vapor Phase Epitaxy on Sapphire Wafers. *J. Cryst. Growth* **2006**, *287*, 586−590.

(46) Kushvaha, S.; Kumar, M. S.; Shukla, A.; Yadav, B.; Singh, D. K.; Jewariya, M.; Ragam, S.; Maurya, K. Structural, Optical and Electronic Properties of Homoepitaxial GaN Nanowalls Grown on GaN Template by Laser Molecular Beam Epitaxy. *RSC Adv.* **2015**, *5*, 87818−87830.

(47) Kuball, M. Raman Spectroscopy of GaN, AlGaN and AlN for Process and Growth Monitoring/Control. *Surf. Interface Anal.* **2001**, *31*, 987−999.

(48) Tripathy, S.; Chua, S.; Chen, P.; Miao, Z. Micro-Raman Investigation of Strain in GaN and Al x Ga 1− x N/GaN Heterostructures Grown on Si (111). *J. Appl. Phys.* **2002**, *92*, 3503−3510.

(49) Goni, A.; Siegle, H.; Syassen, K.; Thomsen, C.; Wagner, J.-M. Effect of Pressure on Optical Phonon Modes and Transverse Effective Charges in GaN and AlN. *Phys. Rev. B: Condens. Matter Mater. Phys.* **2001**, *64*, 035205.

(50) Ko, C.-H.; Chang, S.-J.; Su, Y.-K.; Lan, W.-H.; Chen, J. F.; Kuan, T.-M.; Huang, Y.-C.; Chiang, C.-I.; Webb, J.; Lin, W.-J. On the Carrier Concentration and Hall Mobility in GaN Epilayers. *Jpn. J. Appl. Phys.* **2002**, *41*, L226.

(51) Meister, D.; Böhm, M.; Topf, M.; Kriegseis, W.; Burkhardt, W.; Dirnstorfer, I.; Rösel, S.; Farangis, B.; Meyer, B.; Hoffmann, A.; Siegle, H.; Thomsen, C.; Christen, J.; Bertram, F. A Comparison of the Hall-Effect and Secondary Ion Mass Spectroscopy on the Shallow Oxygen Donor in Unintentionally Doped GaN Films. *J. Appl. Phys.* **2000**, *88*, 1811−1817.

(52) Hwang, C.; Schurman, M.; Mayo, W.; Lu, Y.; Stall, R.; Salagaj, T. Effect of Structural Defects and Chemical Impurities on Hall Mobilities in Low Pressure MOCVD Grown GaN. *J. Electron. Mater.* **1997**, *26*, 243−251.

(53) Wang, T.; Shirahama, T.; Sun, H.; Wang, H.; Bai, J.; Sakai, S.; Misawa, H. Influence of Buffer Layer and Growth Temperature on the Properties of an Undoped GaN Layer Grown on Sapphire Substrate by Metalorganic Chemical Vapor Deposition. *Appl. Phys. Lett.* **2000**, *76*, 2220−2222.

(54) Kordoš, P.; Javorka, P.; Morvic, M.; Betko, J.; Van Hove, J.; Wowchak, A.; Chow, P. Conductivity and Hall-Effect in Highly Resistive GaN Layers. *Appl. Phys. Lett.* **2000**, *76*, 3762−3764.

(55) Xiao, R.; Liao, H.; Cue, N.; Sun, X.; Kwok, H. S. Growth of C-Axis Oriented Gallium Nitride Thin Films on an Amorphous Substrate by the Liquid-Target Pulsed Laser Deposition Technique. *J. Appl. Phys.* **1996**, *80*, 4226−4228.

(56) Klingshirn, C. F. *Semiconductor Optics*; Springer Science & Business Media: Berlin, 2012.

(57) Razeghi, M.; Rogalski, A. Semiconductor Ultraviolet Detectors. *J. Appl. Phys.* **1996**, *79*, 7433−7473.

(58) Ozbay, E.; Biyikli, N.; Kimukin, I.; Kartaloglu, T.; Tut, T.; Aytur, O. High-Performance Solar-Blind Photodetectors Based on Al/sub x/ Ga/sub 1-x/N Heterostructures. *IEEE J. Sel. Top. Quantum Electron.* **2004**, *10*, 742−751.

(59) Kamran, K.; Saeid, K.; Farshid, R.; Fatemeh, K. Highly Sensitive Porous PtSi/Si UV Detector with High Selectivity; *2013 IEEE Regional Symposium on Micro and Nanoelectronics (RSM)*; IEEE, 2013; pp 194−196.

(60) Keramatnejad, K.; Khorramshahi, F.; Khatami, S.; Asl-Soleimani, E. Optimizing UV Detection Properties of N-ZnO Nanowire/P-Si

DOI: 10.1021/acsami.7b03554
ACS Appl. Mater. Interfaces 2017, 9, 21539−21547

Heterojunction Photodetectors by Using a Porous Substrate. *Opt. Quantum Electron.* **2015**, *47*, 1739−1749.
(61) Sun, X.; Li, D.; Jiang, H.; Li, Z.; Song, H.; Chen, Y.; Miao, G. Improved Performance of GaN Metal-Semiconductor-Metal Ultraviolet Detectors by Depositing SiO_2 Nanoparticles on a GaN Surface. *Appl. Phys. Lett.* **2011**, *98*, 121117.
(62) Li, D.; Sun, X.; Song, H.; Li, Z.; Chen, Y.; Miao, G.; Jiang, H. Influence of Threading Dislocations on GaN-Based Metal-Semiconductor-Metal Ultraviolet Photodetectors. *Appl. Phys. Lett.* **2011**, *98*, 011108.
(63) Monroy, E.; Omnès, F.; Calle, F. Wide-Bandgap Semiconductor Ultraviolet Photodetectors. *Semicond. Sci. Technol.* **2003**, *18*, R33−R51.
(64) Marks, R.; Halls, J.; Bradley, D.; Friend, R.; Holmes, A. The Photovoltaic Response in Poly (P-Phenylene Vinylene) Thin-Film Devices. *J. Phys.: Condens. Matter* **1994**, *6*, 1379−1394.

DOI: 10.1021/acsami.7b03554
ACS Appl. Mater. Interfaces 2017, 9, 21539−21547